Dhaka Univ. J. Sci. 74(1): 87-94, 2026 (January)
Prof. M. Muhibur Rahman Memorial Issue
ISSN 1022 - 2502, E-ISSN 2408- 8528
DOI: https://doi.org/10.3329/dujs.v74i1.84350

Vibration Analysis of a Soft Hydrodynamic Manipulator

Sabi Jahan Maliha[1], Tasnemul Hasan Nehal[2], Shugata Ahmed[3*], and Muhammad Hasibul Hasan[4]

[1,3]Department of Robotics and Mechatronics Engineering, Faculty of Engineering and Technology University of Dhaka, Dhaka-1000, Bangladesh
[2]Control and Instrumentation Engineering Department, King Fahd University of Petroleum and Minerals Academic Belt Road, Dhahran 31261, Saudi Arabia
[4]Department of Mechanical and Industrial Engineering, Faculty of Engineering and Architectural Science Ryerson University, Toronto, Canada

(Received : 15 September 2025; Accepted : 1 January 2026)

Abstract

In modern times, industrial automation has made significant progress by reducing human labour and speeding up manufacturing processes. However, limitations in traditional manipulators have led to restricted workspaces and time-consuming repetitive tasks, making the implementation of flexible manipulators with increased freedom highly beneficial. Regardless, the deformation of the soft manipulator poses a challenge to its actuation, resulting in undesired vibrations. Additionally, the actuation process itself, characterised by the utilisation of pumping power, represents a significant factor contributing to the observed vibrations. This research focuses on the deformations and vibration analysis of the soft manipulator through experiments. The vibration is characterised by the ripple factor obtained from the fluctuation of the linear and angular positions with respect to changing velocity and time. Initially, an optimised prototype is constructed based on geometric parameters to maximise deflection. Subsequently, vibration analysis is conducted on the optimised prototype with three different test fluids: water, engine oil, and mustard oil with large viscosity differences at the same temperature, to identify the most suitable fluid in terms of viscosity for actuation. Based on experimental analysis, engine oil is selected as the most suitable fluid due to its deformation capability at low Reynolds numbers, as well as its vibration control characteristics. This optimal fluid is then used for various test scenarios involving the geometric model. Finally, numerical results are validated with experimental data.

Keywords: soft manipulator, deformation, vibration, pumping power, ripple factor

I. Introduction

In the context of the industry 4.0, robotics is transforming the manufacturing landscape, thereby enhancing efficiency to unprecedented levels. Soft robotics, a new area of research, uses flexible materials to excel in complex environments and master the delicate manipulation of objects. It has a wide-ranging impact, from changing the way healthcare[1–4] and manufacturing[5–10] work to making human-robot interactions safer[11–16] as well as exploring maritime industries[17–27].

Soft fluidic actuators are potential candidates for these types of tasks due to their high power-to-weight ratio. Their safety features[28] along with versatile and diverse functions such as soft interactions[29], durability[30 31], inventive design[32 33], and energy efficiency[34], have a huge effect on healthcare, exploration, and many other fields.

Numerous studies have been conducted on the manipulation of objects using soft robots with the objective of reducing cost, achieving the maximum bending angle, increasing speed and precision, and reducing energy consumption. A low-cost bending actuator for flexible robotic applications was proposed by She et al.[35]. The actuator was able to attain a bending angle of 90 degrees and a bending radius of 9.6 mm with a response time of less than 5 seconds, as evidenced by the results. Giannaccini et al.[36] introduced a variable compliance, flexible gripper (VCSG) that is capable of grasping objects of varying shapes and sizes. Shintake et al.[37] developed a soft robotic gripper that is capable of delicate and precise object manipulation. The gripper is made of silicon rubber material and is pneumatically controlled. Manti et al.[38] proposed a bioinspired soft robotic gripper for adaptable and effective grasping. The gripper mimics the functionality of an octopus tentacle, which can adapt its shape to grasp objects of different sizes and shapes. Wang et al.[39] created a flexible gripper that is capable of operating at a rapid pace and consumes minimal energy.

Despite of numerous advantages, soft fluidic actuators encounter obstacles such as vibration[40] and fluid leakage[41]. Current research works did not address vibration modelling, which makes it harder to define control strategies that are needed to make these robots more precise and perform better.

This paper focuses on the vibration analysis of a soft hydrodynamic manipulator through experiments. In this regard, a soft manipulator has been fabricated and a test setup has been developed. Three separate test fluids with large viscosity differences - water, engine oil, and mustard oil, were used in the experiment. The vibration is characterized by ripple factor, calculated from temporal changes in linear and angular displacements in various planes.

[*]Author for correspondence. e-mail: shugataahmed.rme@du.ac.bd

II. Materials and Methods

Experimental setup

A single-link robotic manipulator was fabricated with soft silicon rubber Ecoflex 00-50. The manipulator with all the dimensional parameters is shown in Fig. 1. Dimensional values are given in Table I. A DC pump, connected to the inlet through a 0.5-inch diameter flexible PVC pipe, is used to deliver fluid. The pump motor speed can be controlled by a motor speed controller. Flow rate is measured by a Hall-

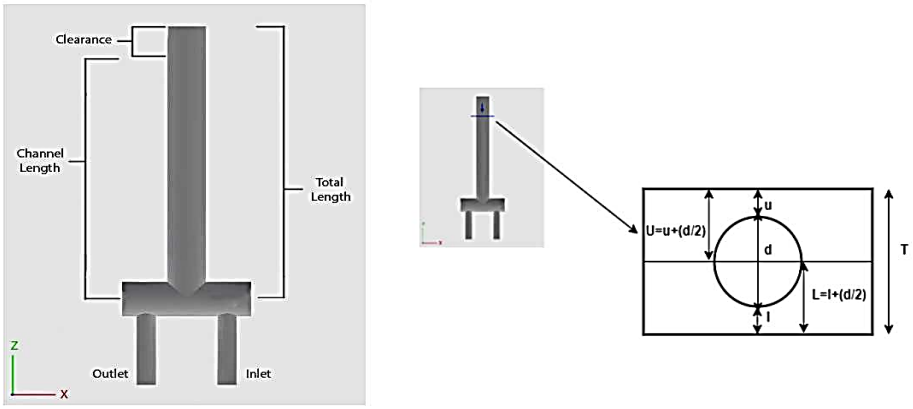

Fig.1. (a) CAD design of the manipulator with external dimensions, (b) CAD design of the manipulator with cross-sectional dimensions.

Dimensional parameters	Values (mm)
Total length (L_t)	94.50
Channel length (L_{ch})	89.15
Clearance (c)	5.35
Channel diameter (d)	12.028
Upper thickness (u)	2.686-3.686
Lower thickness (l)	3.686-4.686
Total thickness (T)	19.4
Inlet and outlet diameter (D)	6
Inlet and outlet channel length (L)	24

Table I. Dimensions of single link robotic manipulator

effect flow meter sensor. The outlet pressure is measured using an electronic industrial pressure sensor. A 10 DOF gyro sensor from SparkFun is used to measure the deflection and acceleration of the manipulator. Among the 10 DOF, three measure acceleration, three for magnetic field, three measure orientation and one is for temperature. However, only accelerations along the X, Y, and Z axes and orientations about the Y and Z axes are useful for this study. The schematic diagram of the setup is shown in Fig. 2.

It is noted that when the channel diameter and total thickness are constant, the ratio of upper to lower thickness is defined as follows:

$$\text{Upper to lower thickness ratio, } \alpha = \frac{u+\frac{d}{2}}{l+\frac{d}{2}} \quad (1)$$

Again, for a constant total thickness, clearance to channel length ratio is defined as:

$$\text{clearance to channel length ratio, } \beta = \frac{cl}{L_{ch}} \quad (2)$$

Finally, channel diameter to total thickness ratio, $\mu = \frac{d}{T}$ (3)

The manipulator is fabricated with optimised α, β, and μ obtained from numerical simulation following equations (1)-(3). However, it is not the scope of this paper. Hence, details are excluded.

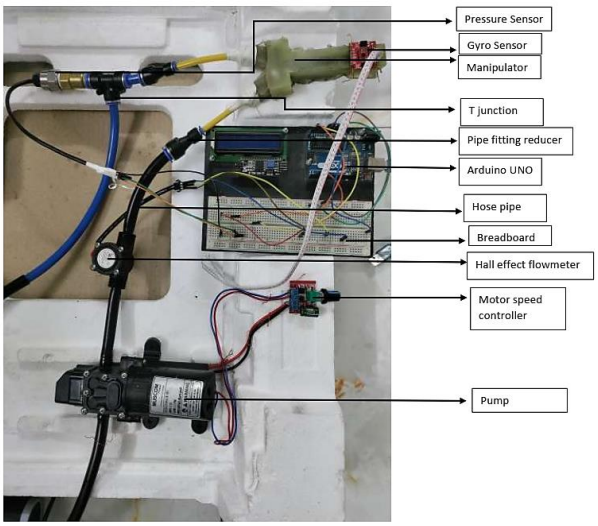

Fig. 2. Schematic diagram of the test setup.

When the fluid flows into the channel through the inlet at a specific flow rate, the manipulator deforms because of the pressure exerted at the outlet. When the outlet pipe is clenched, pressure increases, resulting in higher deflections. In this study, the outlet is fully closed so that maximum pressure develops for a certain flow rate. The bending of

the manipulator body can be represented with the diagram shown in Fig.3.

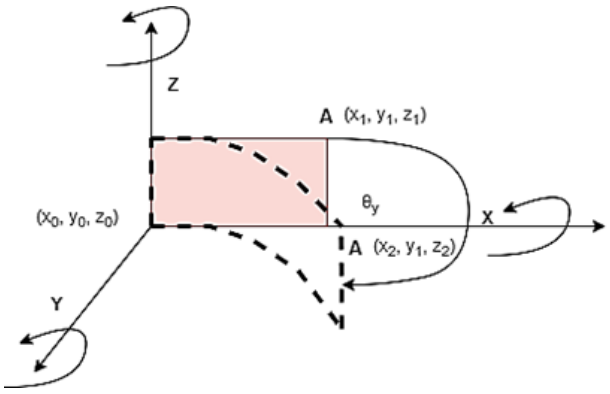

Fig. 3. Illustration of the bending of the manipulator.

The initial position of point A on the manipulator body is A (x_1, y_1, z_1). After bending, the point moves to A (x_2, y_2, z_2). The coordinate values are obtained from gyro sensor from which bending angles θ_y and θ_z are calculated using following equations:

$$\theta_y = tan^{-1}\frac{z_2 - z_1}{x_2 - x_1} \quad (4)$$

$$\theta_z = tan^{-1}\frac{x_2 - x_1}{y_2 - y_1} \quad (5)$$

Vibration analysis

The vibration is characterised by a ripple factor (ϒ). The ripple factor signifies the extent of fluctuation in the amplitude of a periodic waveform. It measures the presence of harmonics or higher-frequency components in the signal. A low ripple factor indicates a more consistent and smoother waveform, whereas a high ripple factor suggests a greater degree of distortion or non-linearity. The ripple factor can be determined by calculating the ratio between the root mean square (RMS) value of the AC component and the DC component of the signal.

If the deflection signal comprises M components, namely X_1, X_2, X_3, ..., X_M, then the AC component of the signal can be represented as X_{rms}, and the DC component of the signal can be represented as X_m.

AC component of the signal, $X_{rms} = \sqrt{\frac{X_1^2 + X_2^2 + \cdots + X_M^2}{M}}$ (6)

DC component of the signal, $X_m = \frac{X_1 + X_2 + \cdots + X_M}{M}$ (7)

So, ripple factor, $\gamma = \frac{X_{rms}}{X_m}$ (8)

III. Results and Discussion

Elasticity analysis

Fig. 4 represents the outlet pressure vs. Reynolds number curve. It can be concluded from the graph that the maximum developed pressure is approximately 2 MPa. This pressure is in the elastic limit of the Ecoflex 00-50.

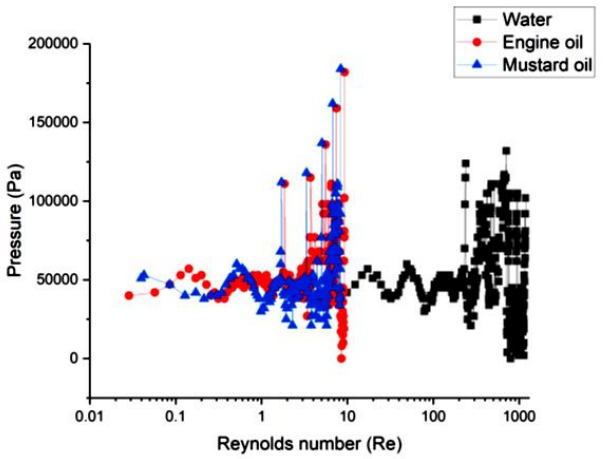

Fig. 4. Pressure vs. Reynolds number.

Vibration analysis in the velocity domain

Fig. 5 represents the linear and angular displacements vs. Reynolds number (Re) plot for three different test fluids. These figures show that water reaches its maximum deflection point at a much higher Reynolds number (Re ≥ 100) than the engine oil (Re = 9.3) and mustard oil (Re = 8.31). After analysing the above results, it can be concluded that, to reach the maximum deflection, the flow rate needs to be high for water because water is less viscous than the other two test fluids.

From Fig. 5, it is observed that in most cases the ripple factor (ϒ) is minimum for either engine oil or the mustard oil. Vibration for displacement along the Z-axis as well as rotation about the Z-axis is well controlled by the mustard oil. In all other cases engine oil shows better performance in vibration control than the other two test fluids.

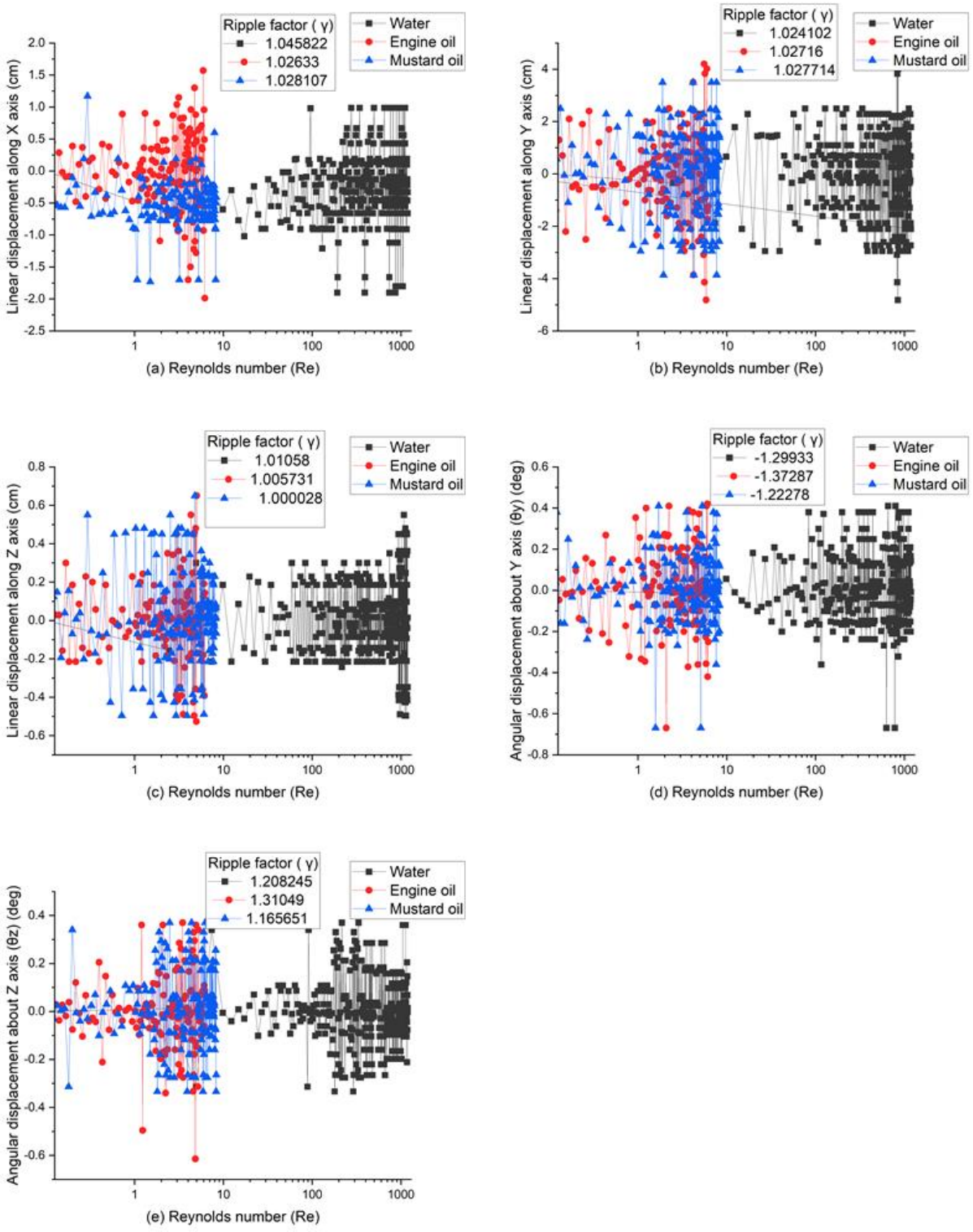

Fig. 5. Displacements vs. Reynolds number (Re) plot for three different test fluids when, α= 0.964, β=0.060, μ= 0.62.

From Fig. 6 it is observed that in most of the cases the ripple factor is minimum for engine oil except for translation along the Z axis, for which at a particular Reynolds number (Re = 9.31), it is minimum for mustard oil. Hence, it can be concluded that among the three test fluids, engine oil and mustard oil are more suitable for deflection as well as vibration control of the manipulator compared to water.

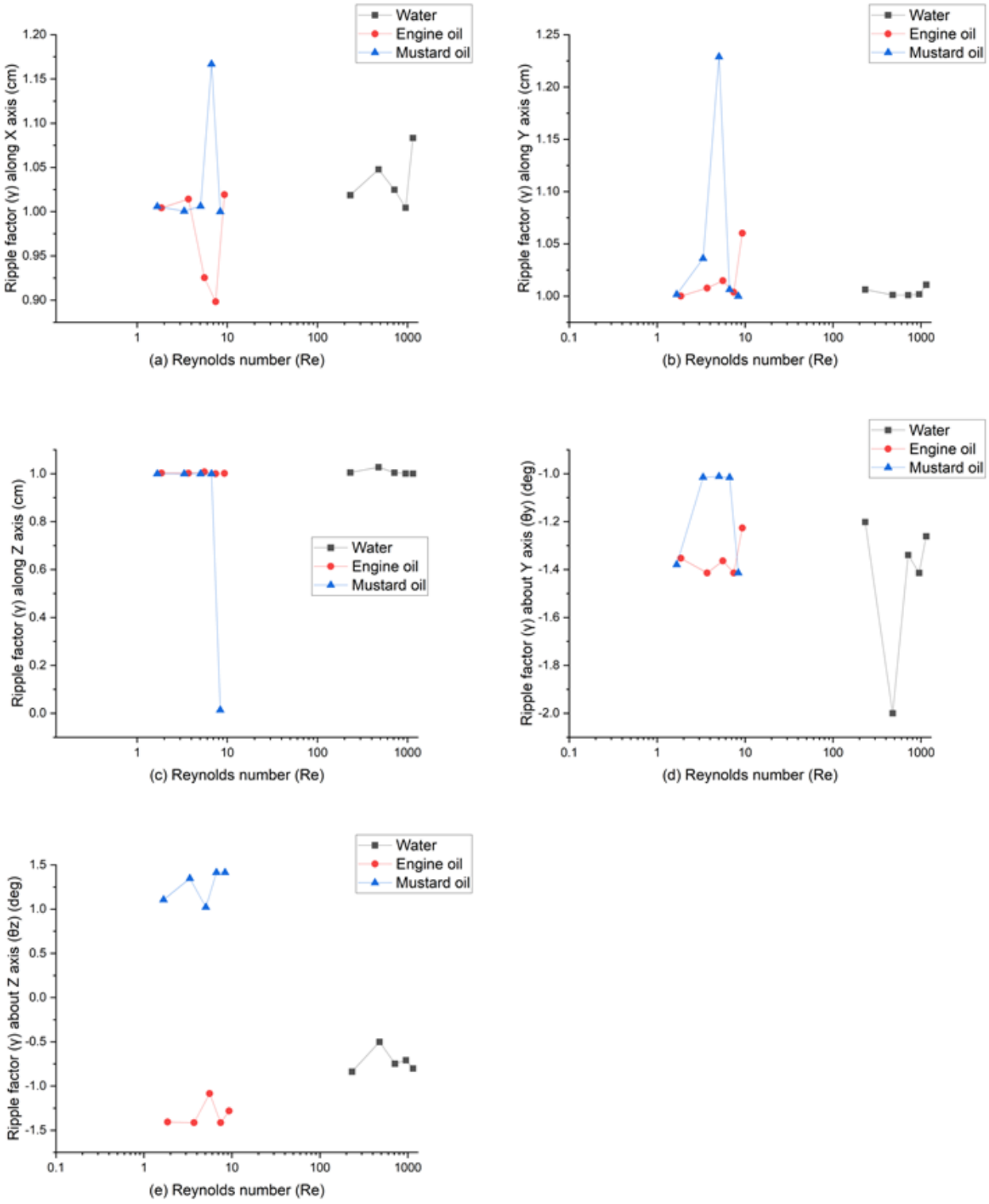

Fig. 6. Ripple factor (ϒ) vs. Reynolds number (Re) plot for three different test fluids when α= 0.964, β= 0.060, μ= 0.62.

Vibration analysis in the time domain

Fig. 7. shows that, in the time domain, minimum ripple factor is obtained for engine oil except displacement and rotation about Z-axis. For later cases, minimum ripple factor is calculated for mustard oil.

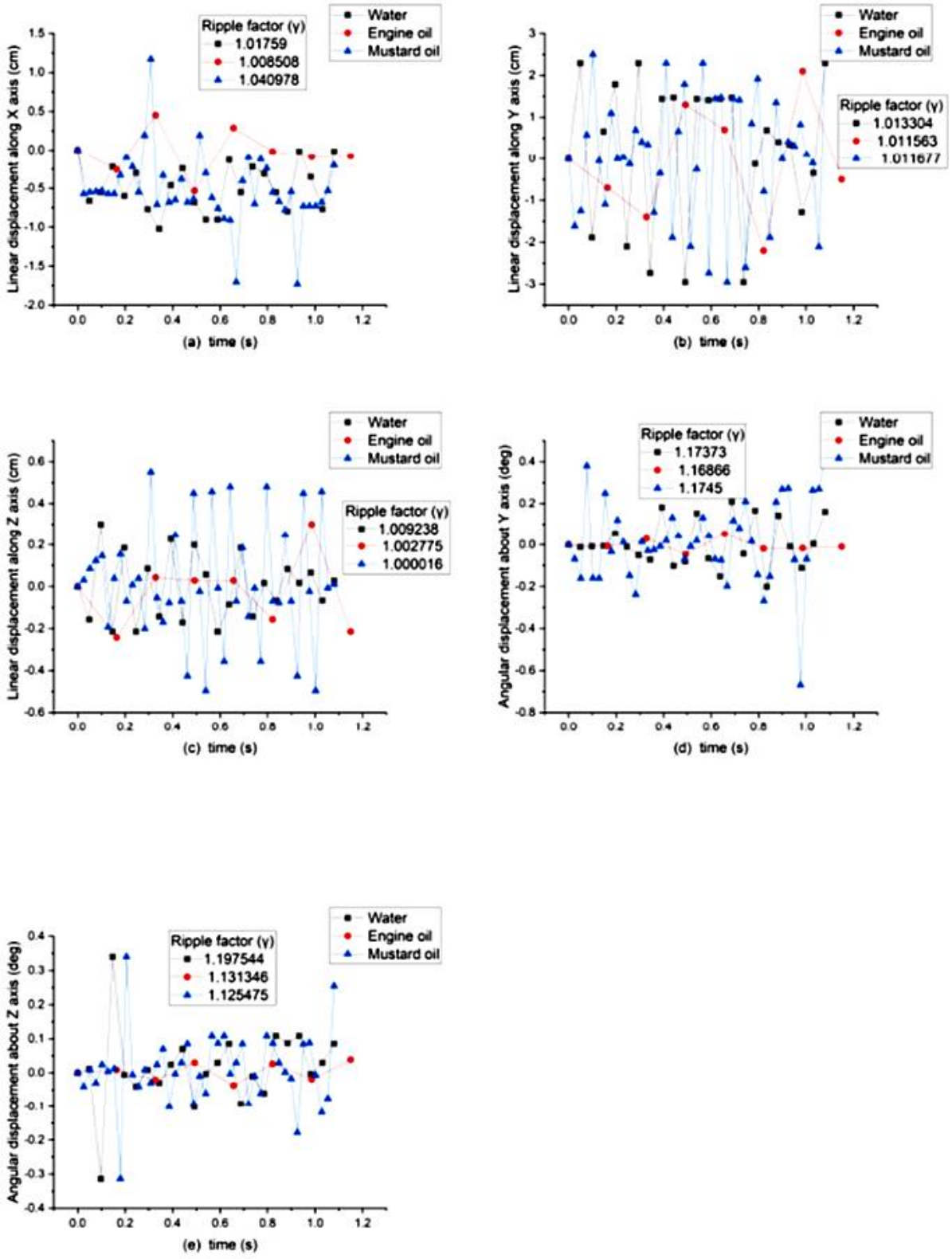

Fig. 7. Displacements vs. time plot for three different test fluids when α= 0.964, β= 0.060, μ= 0.62, Re=6.07.

IV. Conclusions

This study characterises vibrations and explores viscosity's role in control, recommending specific oils. However, challenges exist, including dimensional variations and limited experimental dimensions. Future enhancements involve theoretical modelling, utilising electrorheological and magnetorheological fluids for vibration control, and developing dynamic control systems.

References

1. Cianchetti, M. et al., 2014. Soft robotics technologies to address shortcomings in today's minimally invasive surgery: the stiff-flop approach. Soft robotics 1, 122–131.
2. Sitti, M., 2018. Miniature soft robots—road to the clinic. Nat. Rev. Mater. 3, 74–75.
3. Runciman, M., A. Darzi, and G. P., Mylonas, 2019. Soft robotics in minimally invasive surgery. Soft robotics 6, 423–443.
4. Banerjee, H., Z. T. H. Tse, and H., Ren, 2018. Soft robotics with compliance and adaptation for biomedical applications and forthcoming challenges. Int. J. Robot. Autom 33, 69–80.
5. Ilievski, F., A. D., Mazzeo, R. F., Shepherd, X. Chen, & G. M., Whitesides, 2011. Soft robotics for chemists. Angewandte Chemie Int. Ed.
6. Tse, Z. T. H. et al., 2018. Soft robotics in medical applications. J. Med. Robotics Res. 3, p.1841006.
7. Rossiter, J. M. & H., Hauser, 2016. Soft robotics-the next industrial revolution? IEEE Robotics Autom. Mag. 23, 17–20.
8. Kumar, A., 2018. Methods and materials for smart manufacturing: additive manufacturing, internet of things, flexible sensors and soft robotics. Manuf. Lett. 15, 122–125 (2018).
9. Laschi, C., B. Mazzolai, & M., Cianchetti, 2016. Soft robotics: Technologies and systems pushing the boundaries of robot abilities. Sci. robotics 1, eaah3690.
10. Trivedi, D., C. D., Rahn, W. M. Kier, & I. D., Walker, 2008. Soft robotics: Biological inspiration, state of the art, and future research. Appl. bionics biomechanics 5, 99–117.
11. Park, Y.-L. et al., 2014. Design and control of a bio-inspired soft wearable robotic device for ankle–foot rehabilitation. Bioinspiration & biomimetics 9, p.016007.
12. Polygerinos, P. et al., 2017. Soft robotics: Review of fluid-driven intrinsically soft devices; manufacturing, sensing, control, and applications in human-robot interaction. Adv. Eng. Mater. 19, p.1700016.
13. Jørgensen, J., Bojesen, K. B. & E., Jochum, 2022. Is a soft robot more "natural"? exploring the perception of soft robotics in human–robot interaction. Int. J. Soc. Robotics 14, 95–113.
14. Arnold, T. & M., Scheutz, 2017. The tactile ethics of soft robotics: Designing wisely for human–robot interaction. Soft robotics 4, 81–87.
15. Das, A. & M., Nabi, 2019, "A review on soft robotics: Modeling, control and applications in human-robot interaction" Presented at the International Conference on Computing, Communication, and Intelligent Systems (ICCCIS). October 18-19, Greater Noida, India.
16. Sun, Y.-C., M., Effati, H. E. Naguib, & G., Nejat, 2022. Softsar: The new softer side of socially assistive robots—soft robotics with social human–robot interaction skills. Sensors 23, 432.
17. Youssef, S. M. et al., 2022. Underwater soft robotics: A review of bioinspiration in design, actuation, modeling, and control. Micromachines 13, 110.
18. Der Maur, P. A. et al., 2021, "Roboa: Construction and evaluation of a steerable vine robot for search and rescue applications" Presented at the IEEE 4th International Conference on Soft Robotics (RoboSoft), April 12-16, New Haven, Connecticut, USA.
19. Blumenschein, L. H., L. T., L. T., Gan, J. A., Fan, A. M. Okamura, & E. W., Hawkes, 2018. A tip-extending soft robot enables reconfigurable and deployable antennas. IEEE Robotics Autom. Lett. 3, 949–956.
20. Mintchev, S., D., Zappetti, J. Willemin, & D. A., Floreano, 2018, "Soft robot for random exploration of terrestrial environments" Presented at the IEEE International Conference on Robotics and Automation (ICRA), May 21-25, Brisbane, Australia.
21. Ozkan-Aydin, Y. et al., 2019, "Nutation aids heterogeneous substrate exploration in a robophysical root" Presented at the 2nd IEEE International Conference on Soft Robotics (RoboSoft), April 14-18, 2019, Seoul, South Korea.
22. Elgeneidy, K., N. Lohse, & M., Jackson, 2018. Bending angle prediction and control of soft pneumatic actuators with embedded flex sensors–a data-driven approach. Mechatronics 50, 234–247.
23. Aracri, S. et al., 2021. Soft robots for ocean exploration and offshore operations: A perspective. Soft Robotics 8, 625–639.
24. Subad, R. A. S. I., L. B. Cross, & K., Park, 2021. Soft robotic hands and tactile sensors for underwater robotics. Appl. Mech. 2, 356–382.
25. Zhang, J. et al., 2021, "Dynamic modeling and analysis of underwater swimming snake robot with soft joint" Presented at the ISOPE International Ocean and Polar Engineering Conference, ISOPE–I (ISOPE), June 20–25, Rhodes, Greece.
26. Katzschmann, R. K., J., DelPreto, R. MacCurdy, & D., Rus, 2018. Exploration of underwater life with an acoustically controlled soft robotic fish. Sci. Robotics 3, eaar3449.
27. Gong, Z., J., Hu, K., Cheng, T. Wang, & L., Wen, 2018, "An inverse kinematics method of a soft robotic arm with three-dimensional locomotion for underwater manipulation" Presented at the IEEE International Conference on Soft Robotics (RoboSoft), April 24-28, Livorno, Italy.
28. Majidi, C., 2014. Soft robotics: a perspective—current trends and prospects for the future. Soft robotics 1, 5–11.
29. Teeple, C. B., J. Werfel, & R. J., Wood, 2022, "Multi-dimensional compliance of soft grippers enables gentle interaction with thin, flexible objects". Presented at the International Conference on Robotics and Automation (ICRA), May 23-27, Philadelphia, PA, USA.

30. Thuruthel, T. G., B., Shih, C. Laschi, & M. T., Tolley, 2019. Soft robot perception using embedded soft sensors and recurrent neural networks. Sci. Robotics 4, eaav1488.

31. Preechayasomboon, P. & E., Rombokas, 2021. Sensuator: A hybrid sensor–actuator approach to soft robotic proprioception using recurrent neural networks. In Actuators, vol. 10, 30.

32. Hiller, J. & H., Lipson, 2011. Automatic design and manufacture of soft robots. IEEE Transactions on Robotics 28, 457–466.

33. Stella, F. & J., Hughes, 2023. The science of soft robot design: A review of motivations, methods and enabling technologies. Front. Robotics AI 9, p.1059026.

34. Boyraz, P., G. Runge, & A., Raatz, 2018. An overview of novel actuators for soft robotics. In Actuators, vol. 7, 48.

35. Y. She, J. H. Shi, Chen, and H.-J. Su, 2016. Modeling and validation of a novel bending actuator for soft robotics applications. Soft robotics, **3**, **2**, 71–81.

36. M. E. Giannaccini, I. I. Georgilas, B. Horsfield, A. Peiris, A. G. Lenz, Pipe, and S. Dogramadzi, 2014. A variable compliance, soft gripper. Autonomous Robots, vol. 36, 93–107.

37. J. Shintake, V. Cacucciolo, D. Floreano, and H. Shea, 2018. Soft robotic grippers. Advanced materials, vol. 30, no. 29, p.1707035.

38. M. Manti, T. Hassan, G. Passetti, N. D'Elia, C. Laschi, and M. Cianchetti, 2015. A bioinspired soft robotic gripper for adaptable and effective grasping. Soft Robotics, vol. 2, no. 3, 107–116.

39. Y. Wang, U. Gupta, N. Parulekar, and J. Zhu, 2018. A soft gripper of fast speed and low energy consumption. Science China Technological Sciences, vol. 62, 31–38.

40. H. Jaafar, Z. Mohamed, M. Shamsudin, N. M. Subha, L. Ramli, and A. Abdullahi, 2019. Model reference command shaping for vibration control of multimode flexible systems with application to a double-pendulum overhead crane. Mechanical Systems and Signal Processing, vol. 115, 677–695.

41. Yang, Y., Wu, Y., Li, C., X. Yang, and W., Chen, 2020. Flexible actuators for soft robotics. Advanced Intelligent Systems, **2(1)**, p.1900077.